IN SITU, 23(3), 189–221 (1999)

FACIES-PROPORTION MAPS DERIVED FROM WELL PRODUCTION DATA

A. S. Cullick
Mobil Upstream Strategic Research Center
Dallas, Texas, 75254

C. V. Deutsch
University of Alberta
Edmonton, Alberta, Canada, T6G 2G7

X-H. Wen
Chevron Petroleum Technology Company
La Habra, California,

W. P. Gouveia
Mobil Upstream Strategic Research Center
Dallas, Texas, 75254

ABSTRACT

Previous studies have shown that integration of well production data in geological reservoir modeling can greatly improve the reliability of reservoir performance forecasting by providing more information on the spatial distribution of permeability. The geologic modeling is further enhanced by honoring reservoir facies data derived from well logs and geologic depositional description. Production data can provide an indicator of facies that is tied to the reservoir's performance. This paper presents a new methodology to derive facies-proportion maps from multiple-well, single-phase production data and illustrates how these maps can be utilized for integrated reservoir modeling. A geostatistically based inverse technique, the sequential self-calibration (SSC) method, is used to first generate a series of coarse-scale permeability maps from production data. Facies-proportion maps are then derived from these per-

meability maps through a calibration relationship between facies proportion and effective block permeability. We quantify the uncertainty and illustrate the limitations of the resulting facies-proportion maps due to the non-unique character of both the calibration and the inverted coarse-scale permeability maps.

The facies-proportion maps are to be used along with well petrophysical data, conceptual and descriptive geologic models, as well as seismic data to create fine-scale geostatistical reservoir models for reservoir management. The production data are thus honored indirectly in the final reservoir models.

INTRODUCTION

Production data reflect the responses of the reservoir fluids to the spatial distribution of permeability in the reservoir. Early-time data provide information on near-wellbore heterogeneities; later-time data, particularly the interaction between multiple producing/injecting wells, provide information on heterogeneities throughout the reservoir affected by pressure change. Although production data do not allow unique determination of detailed permeability distribution, valuable information on large-scale trends may be extracted and used for future well placement, injection strategies, and other reservoir-management decisions.

In a previous paper[24], we adapted a sequential self-calibration inversion procedure (SSC)to generate coarse-scale 2D permeability spatial distributions that match well flow rate and pressure data. Often an additional key determinant of reservoir flow behavior is the distribution of reservoir facies, that is, the geometry and connectivity of facies are important for porosity, permeability, and saturation functions such as relative permeability and capillary pressure. Facies maps are often generated from well log and seismic data. In this paper, we present a new method to utilize the production-data-derived permeability to generate estimates of facies proportions. These proportions, tied to the actual reservoir flow responses from wells, can be utilized in building reservoir models that integrate all other available data.

Figure 1 gives a flowchart of the concept developed in this paper:

(A): The dynamic production data at well locations are converted to distributions of coarse-scale permeability, using an inversion method. This

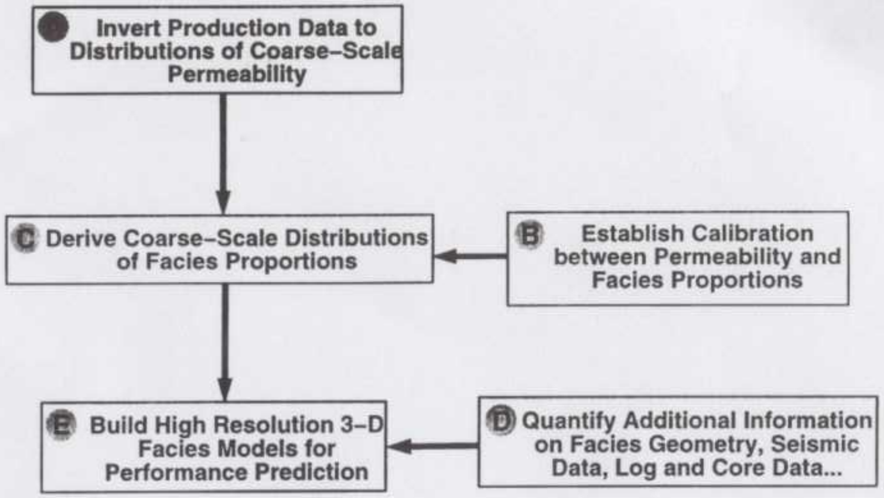

FIG. 1. Flowchart of the concept used in this paper: (A) the dynamic production data at well locations are converted to coarse-scale spatial distribution of permeability using an inversion method, (B) a relationship between permeability and facies proportions is established, (C) the coarse-scale distributions of permeability are transferred to distributions of facies proportions, (D) additional information on the detailed distribution of facies geometries plus other data such as seismic and well data are assembled, and (E) finally, detailed facies-proportion maps are created for reservoir prediction.

inversion is non-unique, that is, there are different realizations of coarse-scale permeability that honor the production data. Notwithstanding this non-uniqueness, the production data constrain the permeability near the wells and interwell where the well production interacts. The result is a probability distribution of coarse-scale permeability at each coarse grid-block location.

(B): The relationship between permeability and facies proportions is established through a calibration exercise. A high-resolution facies model which incorporates core- and well-derived data is upscaled to coarse-scale permeability to directly observe the relationship between facies proportion and permeability (see Figure 2).

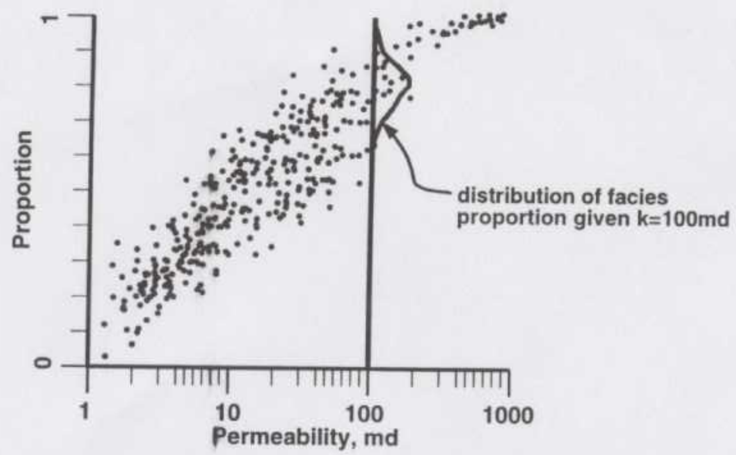

FIG. 2. A schematic illustration of the calibration between permeability and facies proportion. The conditional distributions of facies-proportion are given k=100 shown.

(C): The coarse-scale distributions of permeability are converted to distributions of facies proportions via the calibration relation established in (B).

(D): Additional information on the detailed distribution of facies geometries plus other data such as seismic and well data must be considered in generation of the final reservoir models. These data are assembled and used as input to high-resolution reservoir modeling.

(E): Finally, detailed facies realizations are created for reservoir prediction. These detailed maps use the production-data-derived proportions and all other relevant data.

This procedure permits the dynamic or temporal pressure and rate information at the well locations to be used in facies modeling. The fine-scale 3D facies

models integrate *all* information and are directly useful for reservoir decision making and for constraining high-resolution porosity and permeability models.

The production-data-derived facies proportions are limited to two "lumped" facies: one low-permeability facies and one high-permeability facies. These two "lumped", or "pseudo", facies are distinguished only by separation of their permeability histograms and may lump multiple reservoir or depositional facies which have been identified from other petrophysical properties. Considering more than two facies leads to ambiguous results, that is, a mixture of high and low facies would be indistinguishable from medium-quality facies. In the final high-resolution modeling step, the original reservoir or depositional facies are modeled subject to the proportion constraints imposed by the "lumped" facies.

A calibration approach is taken to relate coarse-scale permeability to facies proportions. This procedure can be outlined as (1) fine-scale facies models are constructed with spatially variable proportions of high and low facies; (2) the effective permeability is calculated by flow simulation using coarse-scale blocks; and (3) a crossplot between facies proportion and effective permeability is constructed. For a given coarse-scale permeability value, we can extract the conditional distribution of the two facies proportions. The higher the permeability, the greater the proportion of high-permeability facies. Figure 2 gives a schematic illustration of a calibration crossplot and the facies proportion distribution for a coarse-gridblock permeability of 100 md. The relation between coarse-scale permeability and facies proportion is non-unique because of the non-constant permeability within the facies and the spatial arrangement of the facies within the coarse blocks. The detailed procedure for calibration will be described later.

There are two sources of uncertainty in the facies proportion maps. First, the effective permeability inferred from the production data is non-unique, i.e., it is not possible to uniquely determine the permeability everywhere using limited production data. We can, however, extract useful spatial trends. Second, as illustrated in Figure 2, the calibration of facies proportion to effective permeability is non-unique. Both of these sources can be quantified allowing us to create a map of the expected facies proportion and the associated uncertainty in facies proportion. We illustrate this with two examples later in the paper.

The coarse-scale facies information derived from production data can be used as a production-data-based check on a conventional or geostatistically derived facies model developed from core, seismic and well log data. But it is better to use the facies proportion maps as an input constraint to build high-resolution 3D facies models. We discuss this procedure and illustrate it with an example.

BACKGROUND

The production data we consider are rate $Q_w(t)$ and pressure $P_w(t)$ as a function of time t at any arbitrary number of well locations, $w = 1, \ldots, n_w$. Production data are non-linearly related to the spatial distribution of reservoir facies and the associated permeability in the reservoir. Establishing constraints on permeability due to production data is an inversion problem that has received considerable attention. The early work of Jacquard and Jain[15] for automatic interpretation of well test data has been followed by many refinements.

A first attempt at a geostatistical approach came in the mid-80's[11]. Reynolds, Oliver, and coworkers[4,20] proposed methods for fast determination of the sensitivity coefficients required in the inversion procedure, and they developed a geostatistically based technique[14,17,18] that generates multiple realizations of reservoir property models.

Landa[16] recently demonstrated additional refinements in the determination of sensitivity coefficients, and Landa and Edoa et al.[9] developed the inversion of parameters describing simple geological shapes, such as channels and distance to channel boundaries. Blanc et al.[2] estimated lithofacies proportions using multiple well-test-derived permeability values on small models. Their method assumes that the permeability for each facies is a constant and that

permeability can be averaged using a power-averaging technique. A stochastic inversion technique, known as the Sequential Self-Calibration (SSC) method, subject to geostatistical constraints, was introduced by Gómez-Hernández and coworkers[3,11]. This method has been shown to be computationally fast and robust[22,27]. The SSC method was adapted by Wen and others[24] to generate coarse-scale permeability maps from production data. In this paper, we apply the SSC method to determine facies-proportion maps.

INVERSION FOR COARSE-SCALE PERMEABILITY

We consider single-phase production data. Techniques that consider multiphase production data remain under development; however, the results of such techniques could be used with the same overall approach[21,25], that is, the conversion of coarse-scale permeability to facies proportions.

The sequential self-calibration (SSC) method, is used to determine 2D coarse-scale spatially correlated permeability fields from the production data (time-dependent rate $Q_w(t)$ and pressure $P_w(t)$ data)[23] . The SSC method is an iterative geostatistically based method coupled with an optimization procedure, which generates multiple equally likely permeability realizations honoring the well production data, yet preserves a given spatial variation structure. Considering the distributions from multiple realizations provides estimates of the uncertainty in the permeability at every location in the reservoir. Typically, the uncertainty will increase away from the well control. The details of the SSC method can be found elsewhere[11,26] and are summarized below.

1. Construct multiple initial permeability realizations that honor as much information as possible, e.g., the permeability histogram and variogram from core data. These initial realizations are initially generated at a coarse scale to allow for inversion (typically fewer than 10,000 blocks). The statistics (e.g., histogram and variogram) for the inversion are also at the coarse scale. It is often necessary to construct a fine-scale realization (the scale of our well data and known statistics), scale it up

to the coarse scale, and extract the needed coarse-scale histogram and variogram. A Gaussian technique such as sequential Gaussian simulation (see the `sgsim` program in GSLIB[7]) has been used in the examples presented later.

Each initial realization is processed one at a time with the following steps.

2. Solve the flow equations with the known well flow rates $Q_w(t)$. The bottomhole pressure $\hat{P}_w(t)$ predicted from the simulator is compared to the observed well pressure $P_w(t)$. An objective function is written that measures the squared difference between the predicted and observed pressures:

$$O = \sum_w \sum_t \left[\hat{P}_w(t) - P_w(t)\right]^2$$

The goal is to minimize this objective function. A gradient-based method will be used, which requires "sensitivity coefficients," that is, the derivative of pressure with respect to the change of each coarse-scale permeability:

$$\frac{\partial \hat{P}_w(t)}{\partial \triangle K_i}, \quad i = 1, \ldots, N$$

where N could be the number of coarse blocks in the model. In practice, N is reduced to about 1/100 of the number of coarse blocks by using the "master-point" concept[11,19]. Optimal changes to permeability are determined for these "master points" and then smoothly interpolated to all coarse gridblocks in the realization.

The sensitivity coefficients are calculated as part of the solution of the flow equations. Most other calculation techniques are too slow for practical implementation.

3. Establish optimal perturbations to the permeability at all master locations with a modified gradient projection method. This "inner optimization" determines the change to the permeability at each master-point location that would lead to more closely matching the pressure data at all wells at all time lags.

The optimal permeability perturbations at the master-point locations are smoothly propagated to all grid nodes by kriging the changes at the master-point locations using the coarse-scale variogram.

4. Return to step 2 until the objective function has been lowered sufficiently close to zero. Fewer than 20 iterations are normally required.

The next step is to convert these distributions of permeability into distributions of facies proportions. For this, we need to have a relationship between facies proportion and effective permeability at the coarse scale.

CALIBRATION OF FACIES PROPORTION WITH EFFECTIVE PERMEABILITY

The relationship between facies proportion and effective permeability can be established using the following calibration procedure.

- Construct a fine-scale detailed facies distribution (a lumped "high- permeability" and a lumped "low-permeability" facies associations only) with appropriate pixel- or object-based facies modeling techniques. This detailed facies distribution could be generated to honor available core, well log, and seismic data.

  The fine-scale facies distribution also accounts for differences in the geometry and continuity of each specific facies. Moreover, it is made up of the original sedimentological facies and not the "lumped" petrophysical facies. The calibration relationship, however, relates the "lumped" facies to coarse-scale permeability with some loss of information.

  Multiple realizations could be considered to ensure a reliable calibration. As illustrated schematically in Figure 2, there should be sufficient calibration points to define the bivariate relationship between facies proportion and effective permeability.

- Fill the fine-scale facies distributions with permeability honoring the core-measured histograms, using a geostatistical technique. In general, the permeability within each "lumped" facies has variability that must be accounted for. The ability to discern the facies will depend on the overlap of the two histograms of permeability – the less overlap the better.

- Overlay a 2D coarse grid aligned with the grid used for the SSC inversion and compute (1) the facies proportion and (2) the effective horizontal permeability of each coarse block. The proportion and effective permeability are calculated from the fine-grid model. A flow-based scale-up technique or, perhaps, a faster power-averaging method could be used to compute the effective block permeability from the fine-scale permeability[5,7,26]. Repeat this for all calibration realizations.
- Crossplot the pairs of facies-proportion and effective permeability values obtained from the calibration realizations. For any effective permeability we now have the conditional distribution of possible facies proportions.

FACIES-PROPORTION MAPS

The facies-proportion maps are read from the calibration relation using the coarse-scale permeability maps (obtained from the SSC inversion). The procedure may be summarized by the following steps:

- For each coarse block, there are L permeability values ($K_i, i = 1, \dots, L$) from the L permeability realizations derived from the SSC inversion.
- For each permeability value ($K_i, i = 1, \dots, L$), we retain all possible facies proportions that fall within a narrow window $[K_i - \Delta K, K_i + \Delta K]$ from the calibrated relationship of facies proportion ($P_i^j, j = 1, \dots, N_i$) and effective permeability.
- All facies-proportion values are then combined into a histogram of possible facies proportions at each location. The local distributions of facies proportions may be summarized by local mean and variance values. We can also plot the probability of exceeding some critical proportion of facies.

In the next section, we demonstrate applications of the proposed methodology using synthetic data sets. The sensitivity of results on the distributions of facies permeability is also investigated.

FIRST EXAMPLE - FLUVIAL RESERVOIR

Consider a fluvial reservoir whose heterogeneity is dominated by the distribution of high-permeability channel sand within a background of low permeability floodplain shales. A reference facies model was constructed by **fluvsim**[8]; an isometric view of that reference model is shown in Figure 3. The permeability of the fluvial channel sand and floodplain shale are constant at 1000 md and 1 md, respectively. Historical production data were simulated assuming single-phase steady-state slightly compressible flow using three wells at locations shown on the 3D fine-scale model (W1, W2, W3 in Figure 3). The rate and pressure data (see Figure 4) are used to infer the proportion of channel sand facies.

The production data shown in Figure 4 are more like a multiple-well interference test than conventional production data. This imposed "interference" between the wells helps to resolve details between the wells. Continuous production of all wells simultaneously provides less information between the well locations.

A 2D map of the reference sand proportion and the upscaled permeability are shown in Figure 5. The global proportion of channel sand in the model is 0.50. The crossplot of the sand proportion versus coarse-scale permeability (see Figure 6) will be used for calibration only. This calibration relationship was constructed by (1) generating a fine-scale facies distribution, (2) populating the facies with porosity and permeability, (3) upscaling with a single-phase pressure solver, and (4) building the calibration crossplot.

Based on the simulated production data and the histogram and variogram of the coarse-scale permeability values, the SSC method was used to construct multiple realizations of coarse-scale permeability. Figure 7 shows the first four realizations in which the production data are matched. The added variability

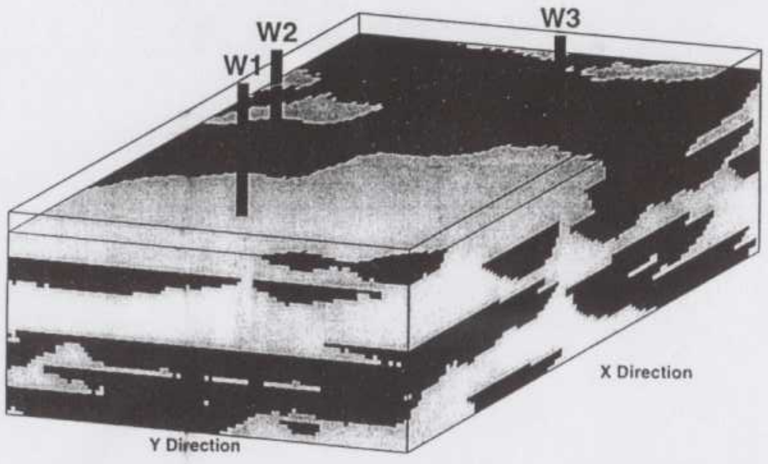

FIG. 3. An isometric view of the reference fluvial model. The high-permeability fluvial channel facies (darker color) are embedded within low-permeability floodplain shales.

of these realizations relative to the reference truth image is due to the lack of an explicit variogram constraint in the SSC algorithm; the variogram is used indirectly. The pressure match for one realization is given in Figure 4. Two hundred realizations of coarse-scale permeability were constructed. To summarize the results, the ensemble-averaged (mean) permeability field and the corresponding variance field are shown in Figure 8.

The sand-proportion for each coarse block can then be computed using the procedure described above. The relationship between permeability and facies proportion (Figure 6) has little spread; therefore, the sand-proportion maps look very similar to the permeability maps. After conversion, Figure 9 shows the ensemble mean proportion and a crossplot of the true proportion and estimated proportion. The regions of low and high sand proportion have been identified as compared to the true proportions in Figure 5. There are regions of indeterminate sand proportion not between the well locations.

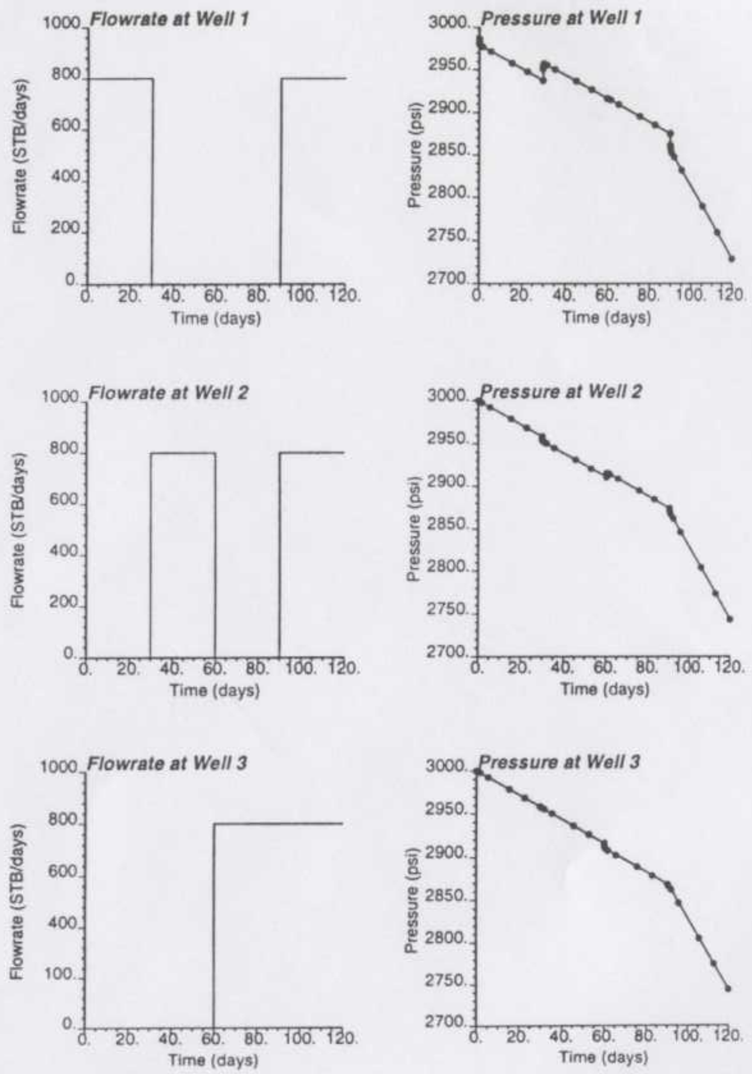

FIG. 4. Production rates and pressure responses at the three wells. The pressure match for one permeability realization generated by the SSC method is also shown by solid circles on the right-side figures.

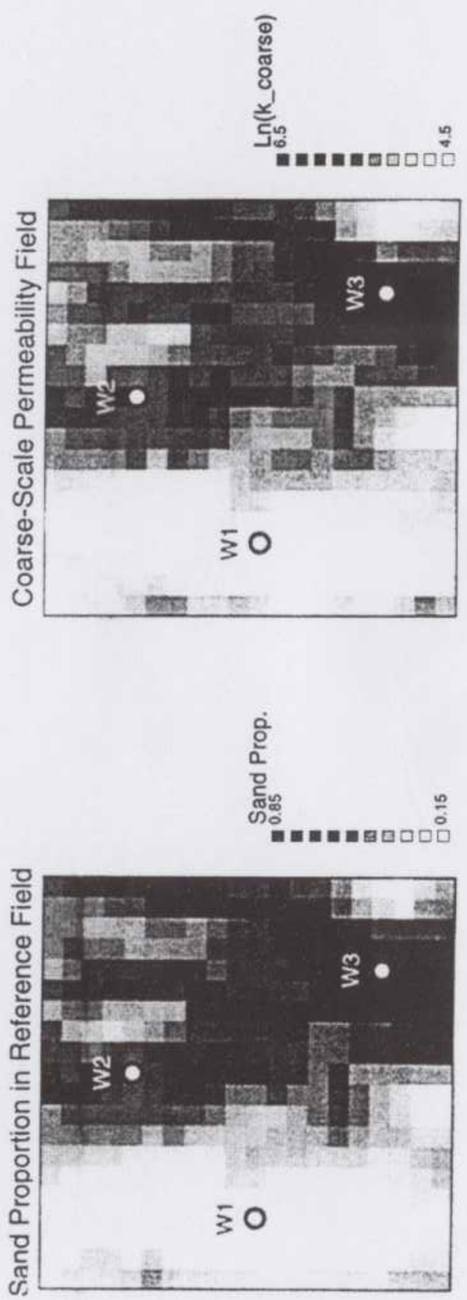

FIG. 5. Proportion of sand from the reference model and the upscaled coarse-scale permeability field (used for calibration only – historical production data taken from fine-scale model)

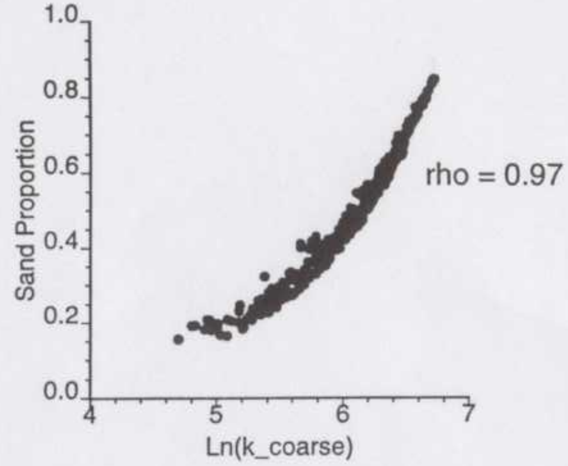

FIG. 6. Crossplot of sand proportion and upscaled permeability. Note the logarithmic scale on the permeability axis.

To show the value of more production data, we take the production data from 20 wells and repeat the entire procedure. The first realization of the SSC inversion is shown in the upper left of Figure 10. The final ensemble mean and variance of the sand proportion are shown on the lower left and lower right of Figure 10, respectively. The crossplot between the true sand proportion and the estimated sand proportion, shown in the upper right of Figure 10, indicates the added value (more accuracy with less uncertainty) of using more production data. Note the improved correlation and the greater spatial resolution on facies proportion (compare with Figure 9).

SECOND EXAMPLE - CARBONATE RESERVOIR

The facies in this second example have less spatial correlation and more within- facies variances of permeability. The 2D reference distributions of facies and permeability are shown in Figure 11. The "patchy" spatial distribution of facies is more representative of a reservoir with a strong diagenetic

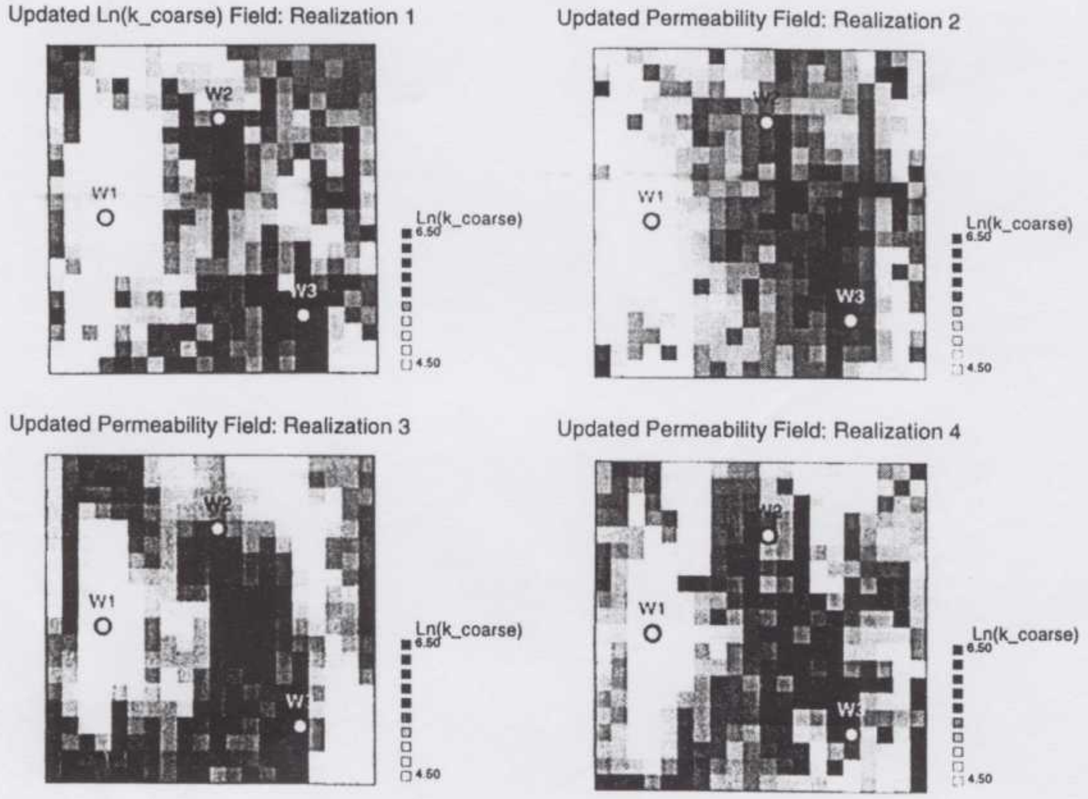

FIG. 7. Four coarse-scale realizations of permeability that match production

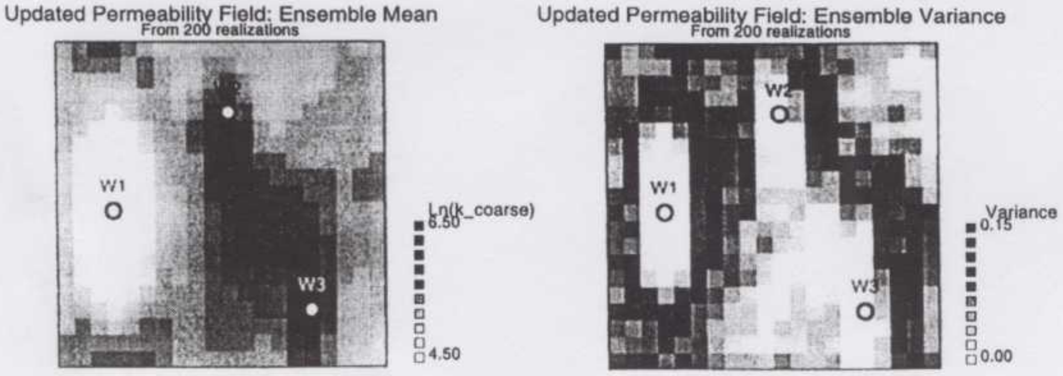

FIG. 8. The ensemble-averaged mean and variance of the coarse-scale permeability computed from 200 realizations.

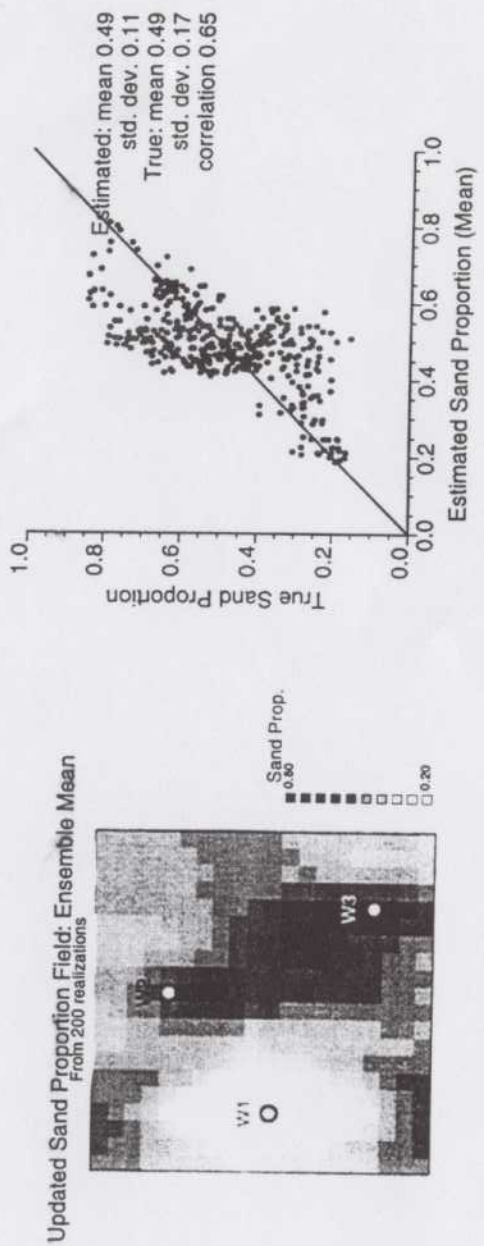

FIG. 9. The ensemble-averaged mean facies proportion and a crossplot between the true sand proportion (from the original 3D fluvial model) and estimated sand proportion (average of 200 realizations).

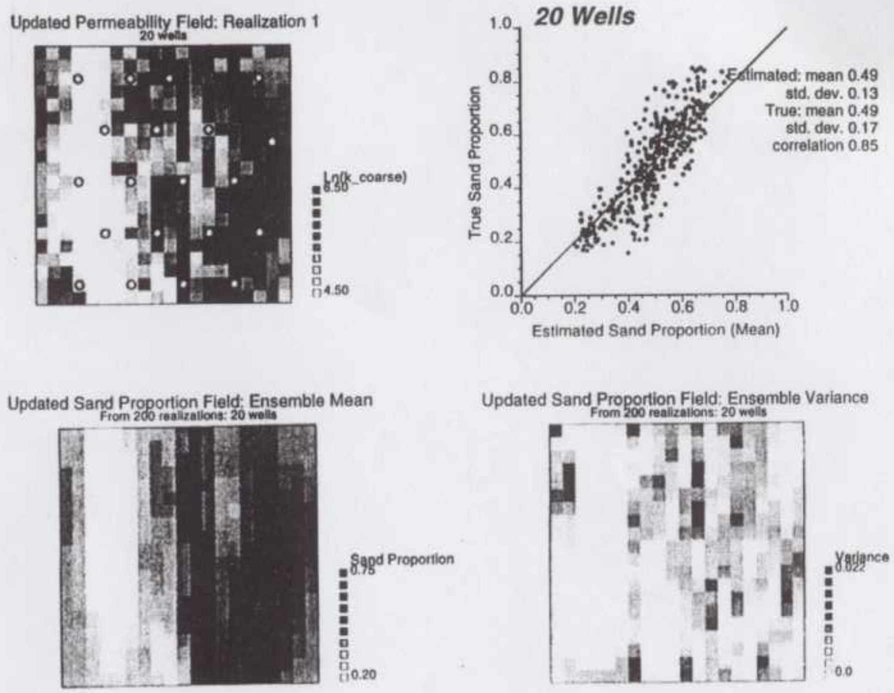

FIG. 10. The results when production data for 20 wells are used. One realization of the SSC inversion is shown in the upper left. The final ensemble mean and variance of the sand proportion are shown at the lower left and lower right, respectively. The crossplot between the true sand proportion and the estimated sand proportion is shown at the upper right.

overprint, such as a carbonate reservoir. This reservoir model was generated by sequential indicator simulation to have 70% high-permeability facies.

The base reference-case histograms of permeability in the "high" and "low" permeability facies are shown in Figure 12. The histogram of permeability no longer shows the distinct bimodal character after scale-up to the coarse-grid size (see right of Figure 12). Although the high- and low-permeability now overlap significantly, there is still valuable information on the facies pro-

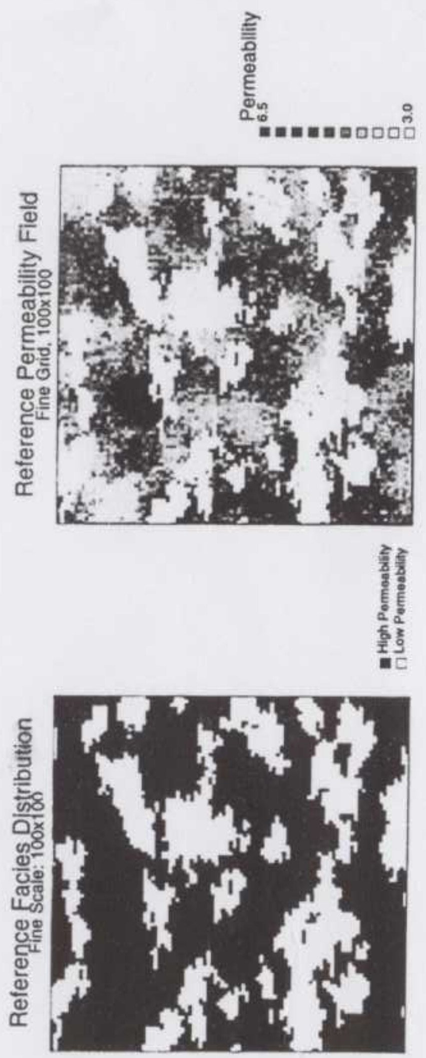

FIG. 11. Reference facies and fine-scale permeability distributions for the second example.

portions. Figure 13 shows the reference coarse-scale facies proportion map (obtained from the fine-scale reference facies map) and permeability map (obtained by scaling up the fine-scale reference permeability field) together with a crossplot between the two for calibration. This calibration crossplot tells us that the coarse-scale permeability is largely a function of the facies.

The procedure proposed in this paper was followed to generate facies proportion maps, i.e., (1) the intermediate coarse-scale permeability maps were generated using successively three wells and 20 wells of production data, (2) they were converted to facies proportions using the calibration relationship, and (3) the facies maps were checked for correspondence with the truth (known in this synthetic example). Figure 14 summarizes the results by crossplotting the true proportion and estimated mean proportion using three wells and 20 wells of production data. Note that the correlation between the true and estimated mean proportion is poor, mainly because the facies have non-zero variance and a smaller range of correlation. As expected, there is some improvement when there are 20 wells.

The quality of the areal facies-proportion maps depends on the histograms of permeability within the high- and low-permeability facies. As a sensitivity case, the inversion/calibration was repeated with distributions of permeability that now overlap (see Figure 15). The calibration crossplot now has more uncertainty (see Figure 16). Repeating the procedure (permeability $\longrightarrow$ proportion maps) leads to the results in Figure 17. As expected, the results are systematically poorer than the results from the base case (Figure 14). In the extreme, with completely overlapping permeability distributions, there would be no possible facies resolution from the production data alone. This example also points out that when the reservoir facies have significant variations at a scale less than the coarse-scale representation, then the facies-specific permeabilities get averaged out at the coarse scale corresponding to production data. The estimation of individual facies proportions is then subject to increased error.

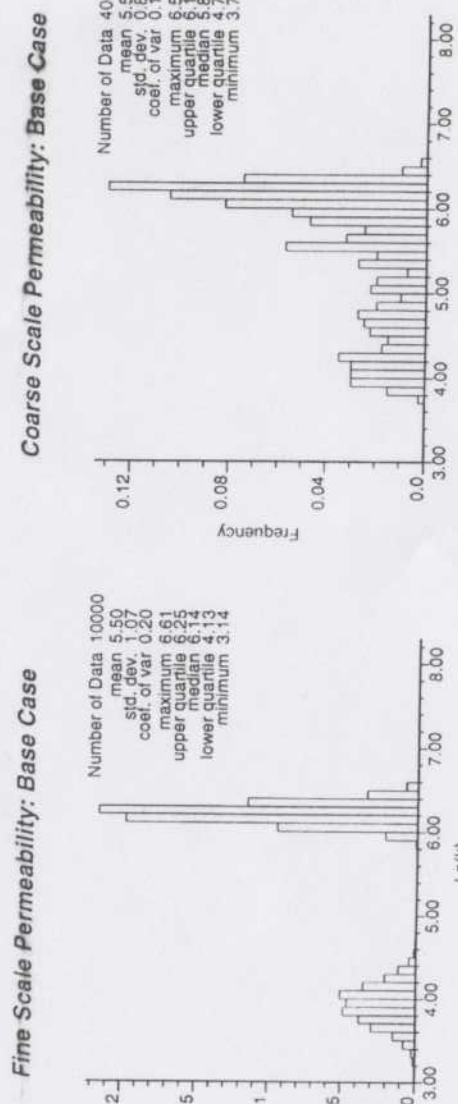

FIG. 12. Histogram of fine-scale and coarse-scale permeability calculated from reference image.

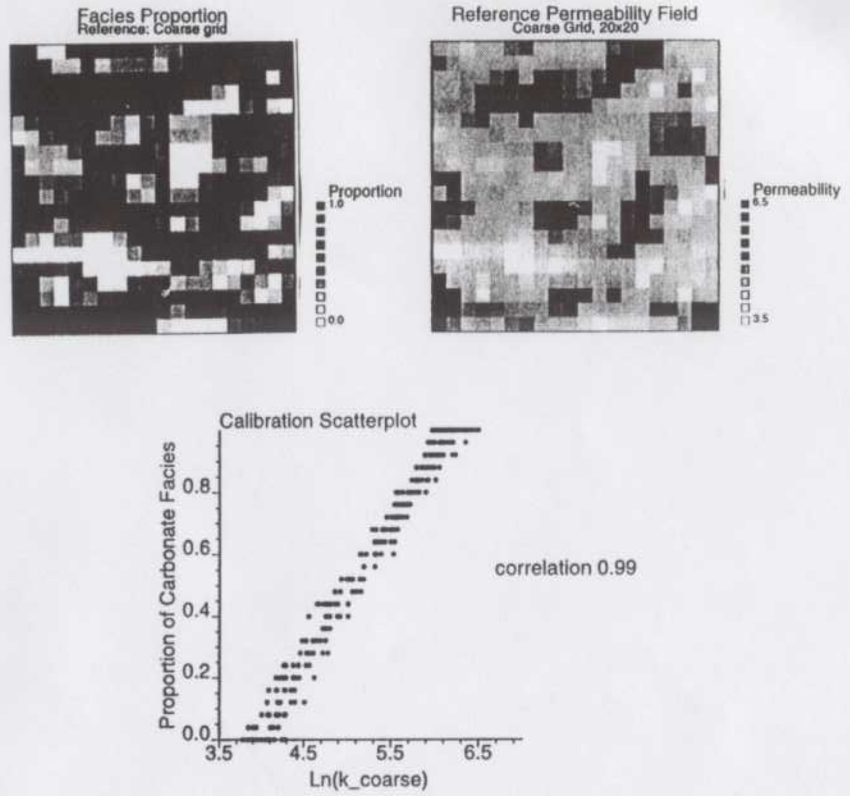

FIG. 13. Reference coarse-scale facies proportion map and permeability map together with crossplot between the two for calibration.

INTEGRATING FACIES-PROPORTION MAPS FOR RESERVOIR MODELING

The facies-proportion maps could be used to guide the location of new wells or to assess areal sweep efficiency. However, in general, these maps are too coarse. The intent of these maps is thus for use as constraints for creating more detailed geostatistical facies models that integrate additional data from seismic and detailed well logs and cores.

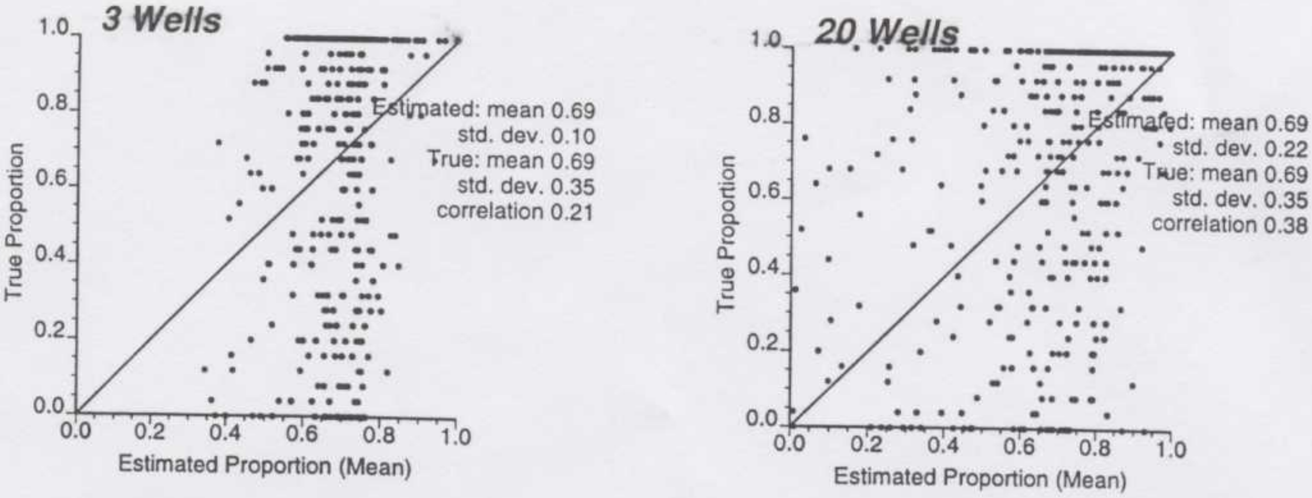

FIG. 14. Crossplot of true proportion and estimated mean proportion using three wells and 20 wells of production data.

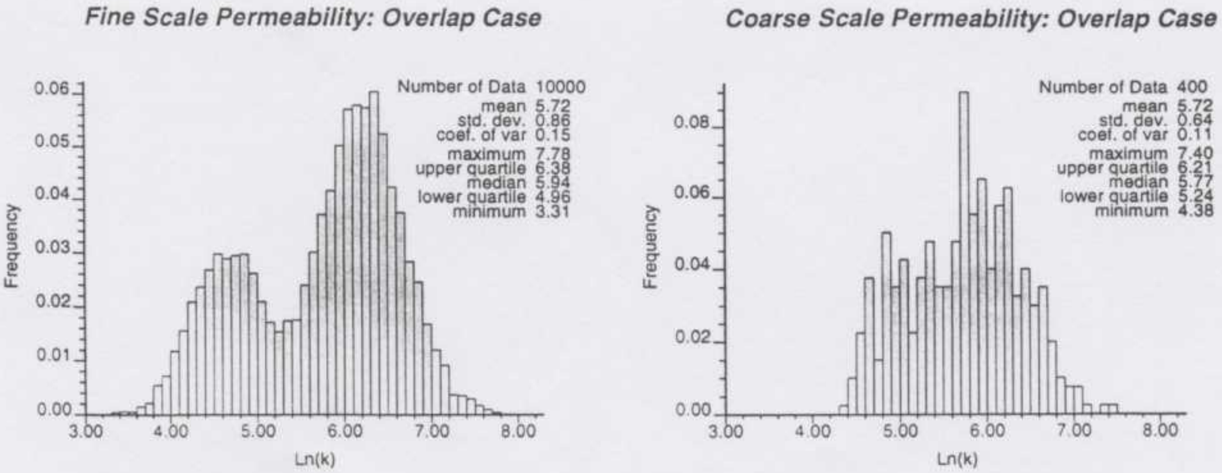

FIG. 15. Histograms of fine-scale and coarse-scale permeability calculated considering facies that overlap.

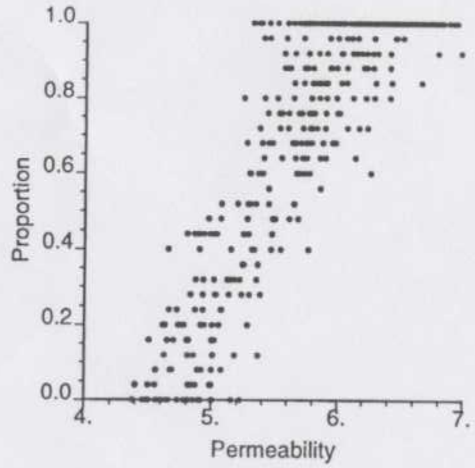

FIG. 16. Calibration crossplot using the "overlap" distributions of permeability. Note that the calibration has greater variability than the base case (Figure 13).

Many facies-modeling techniques permit the use of locally varying proportions. This flexibility was added originally to use seismic data and geological trends, which can also be used to account for production-data-derived proportions. A promising technique to integrate the facies-proportion maps with other data sources is to formulate a multicomponent objective function that is solved by minimizing the model and data misfit through stochastic optimization[5]. The essence of the method is to minimize the misfit between the model and the input facies proportions derived from well logs, core, seismic, production data, and geologists' conceptual maps, while honoring the resolution and uncertainty of each of the data types. The facies-proportion-related components of the objective function are summarized elsewhere[5].

Well data are used to constrain the global proportion and depth proportion of each lithofacies type. Additional data from variogram analysis or facies transition probabilities[5] can be included. Facies proportions from production data and seismic inversion can take the form of unidimensional probability density functions (PDFs) at the scale of the coarse grid. These proportions

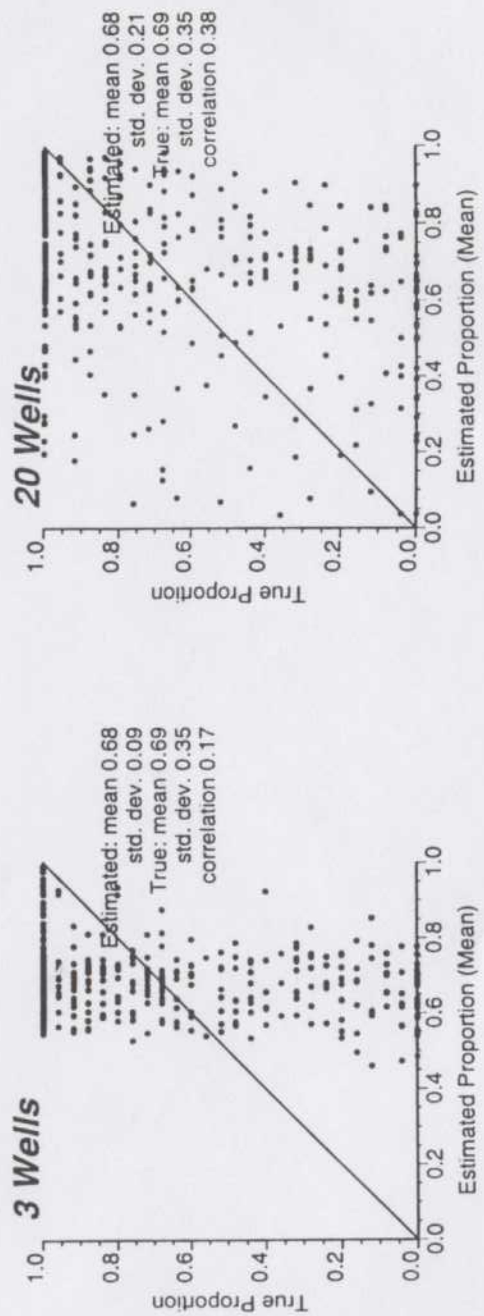

FIG. 17. Crossplot of true proportion and estimated mean proportion using three wells and 20 wells of production data using the "overlap" distributions of permeability.

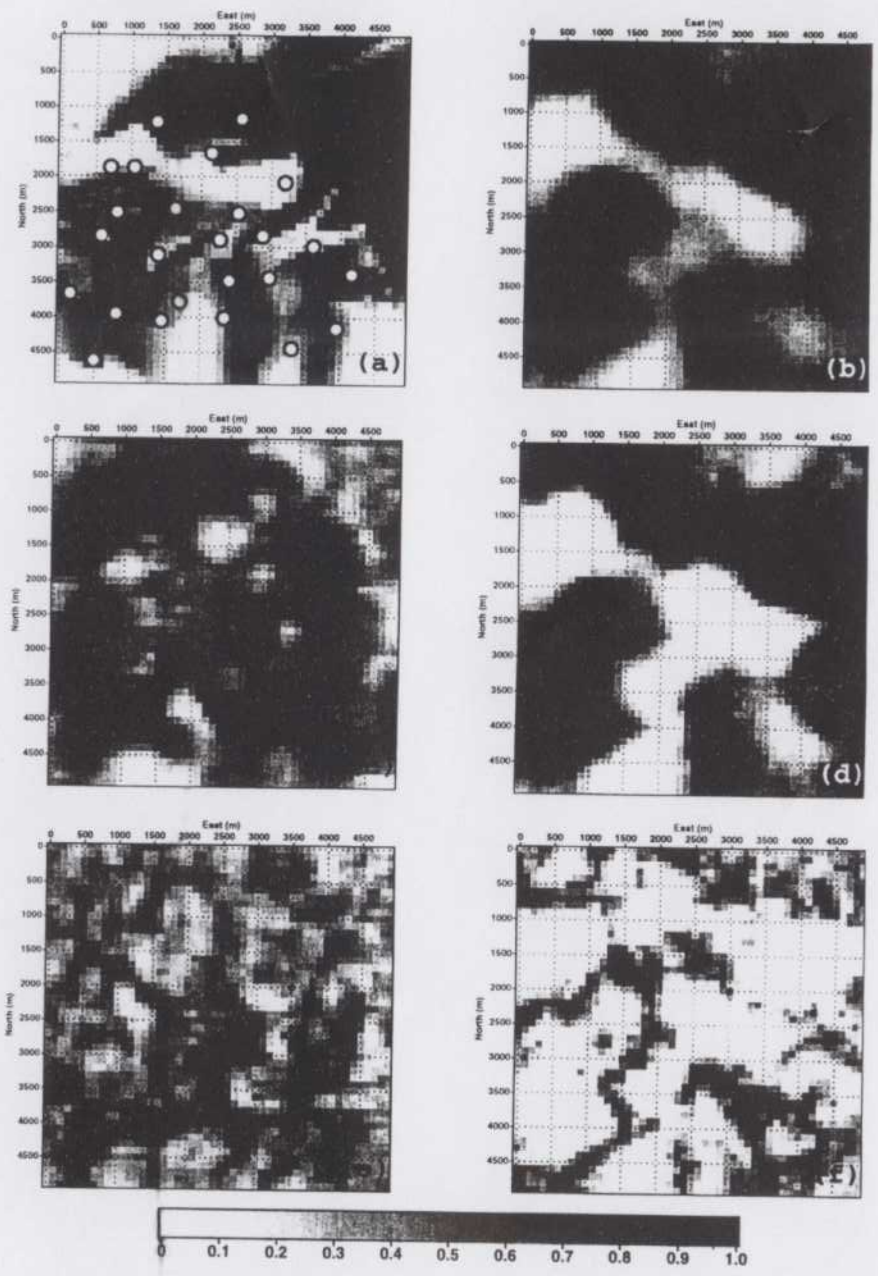

are honored on the fine-scale realizations via a quantile-matching outlined by Deutsch[6]. Figure 18 presents an example of the results from one such data-integration exercise that used production-data-derived facies proportions to build a reservoir model. The reference data model is a 3D volume map of six lithofacies, each with associated porosity and permeability. The model is 100 $\times 100 \times 10$ grid cells of approximate dimensions 5 km $\times$ 5 km $\times$ 60 m. There are six lithofacies in the reference model, two labelled as "low" permeability facies and four labelled as "high" permeability facies. There are 25 wells with 10 facies measurements per well distributed within the model. Figure 18a is the 2D map of the facies proportions at each x,y grid location for the reference model and the well locations. Figures 18b, c, and d show the mean facies proportions for 50 realizations each, using various data in the stochastic optimization. Figure 18b shows the facies proportions derived from production data alone using the SSC method. Figure 18c shows the facies proportions derived from the well data, variograms, and facies transition probabilities with no production data. Figure 18d is the facies proportions with the addition of the production-data-derived proportions with well proportions and transition probabilities. Figures 18e and f are the variances of the proportions from 200 realizations without and with production data, respectively. A comparison of Figure 18d with Figure 18a shows that most areas of high- and low-permeability facies are improved with the data integration.

Other geostatistical methods can also utilize production-data-derived facies proportions to generate better constrained detailed reservoir models include truncated Gaussian simulation[7,28], sequential indicator simulation[1,7], and object-based modeling techniques[8,13].

FIG. 18. Example of using production-data-derived facies proportions to build a reservoir model. (a) reference facies proportions with well locations; (b) mean from production data alone(SSC); (c) mean from well data, variograms, transition probabilities; (d) mean with all from (c) and production-data-derived proportions; (e) variance with no production data; (f) variance with production data

DISCUSSION AND CONCLUSIONS

One outstanding challenge in reservoir characterization is understanding the constraints on the spatial distribution of facies that can be provided by well production data. The methodology presented in this paper provides a tool to guide facies mapping using single-phase multiple-well production data. This is the type of data available in primary depletion and before water breakthrough, that is, early in the life of a reservoir. A number of important reservoir management decisions have to be made during these early stages and our methodology should be useful. The use of multiphase production data remains an important and active area of research.

Two examples were presented to demonstrate the efficacy of the proposed methodology. The SSC method establishes multiple realizations of coarse-scale permeability that, with the aid of a calibration, can be translated into constraints on the proportion of facies. Comparing the results with three wells and 20 wells illustrated the value of more production data.

The two examples illustrated the limitations of the approach: (1) it is limited to considering two petrophysical facies groups, low- and high-permeability facies, (2) the calibration depends on the overlap of the permeability histograms between the lumped facies, and (3) the inversion of production data to permeability is done in two dimensions not accounting for permeability anisotropy; such anisotropy must be introduced in the downscaling to fine-scale facies, porosity and permeability.

The examples also provided some rules of thumb for the conditions under which to expect reasonably good estimates of the coarse-scale facies proportion, i.e., low standard deviation and high correlation between true proportion and estimated proportion. The conditions are that the core-measured permeability histograms have little overlap and the areal extent of reservoir facies is on the scale of the coarse-scale representation. These conditions exist for the fluvial example and for many siliciclastic environments for which there are large-scale pay and non-pay facies (fluvial channel systems, lower shoreface, deep-water channel-levee, and deep-water fan-lobe complexes).

ACKNOWLEDGEMENTS

The authors thank the Stanford Center for Reservoir Forecasting and Mobil Technology Company for sponsoring this research.

REFERENCES

[1] F. G. Alabert and G. J. Massonnat. Heterogeneity in a complex turbiditic reservoir: Stochastic modelling of facies and petrophysical variability. In *65th Annual Technical Conference and Exhibition*, pages 775–790. Society of Petroleum Engineers, September 1990. SPE Paper Number 20604.

[2] G. Blanc, L. Y. Hu, and B. Noetinger. Estimation of lithofacies proportions using well and well test data. *SPEREE*, 1 (1), 1998.

[3] J. E. Capilla, J. J. Gómez-Hernández, and A. Sahuquillo. Stochastic simulation of transmissivity fields conditioning to both transmissivity and piezometric data, 2. demonstration in a synthetic case. *Journal of Hydrology*, 203:175–188, 1998.

[4] L. Chu, A. C. Reynolds, and D. S. Oliver. Computation of sensitivity coefficients for conditioning the permeability field to well-test pressure data. *In Situ*, 19(2):179–223, 1995.

[5] C. V. Deutsch. Conditioning reservoir models to well test information. In *Geostatistics-Troia*, volume 1, A. Soares, editor, pages 505–518. Kluwer, Dordrecht, Holland, 1993.

[6] C. V. Deutsch. Direct assessment of accuracy and precision. In *5th International Geostatistics Congress*, Wollongong, Australia, 1996.

[7] C. V. Deutsch and A. G. Journel. *GSLIB: Geostatistical Software Library and User's Guide*. Oxford University Press, New York, 1992.

[8] C. V. Deutsch and L. Wang. Hierarchical object-based stochastic modeling of fluvial reservoirs. *Math Geology*, 28(7):857–880, 1996.

[9] P. F. Edoa, M. Masmoudi, and D. Rahon. Inversion of geological shapes in reservoir engineering using well tests and history matching of production data. In *1997 SPE Annual Technical Conference and Exhibition*, Dallas, TX, October 1997. Society of Petroleum Engineers. SPE Paper Number 38656.

[10] G. Fasanino, J.-E. Molinard, G. de Marsily, and V. Pelcé. Inverse modeling in gas reservoirs. In *1986 SPE Annual Technical Conference and*

Exhibition, New Orleans, LA, October 1986. Society of Petroleum Engineers. SPE Paper Number 15592.

[11] J. J. Gómez-Hernández, A. Sahuquillo, and J. E. Capilla. Stochastic simulation of transmissivity fields conditional to both transmissivity and piezometric data, 1. The theory. *J. of Hydrology*, 203:162–174, 1998.

[12] W. P. Gouveia, A. S. Cullick, and C. V. Deutsch. An optimization framework for reservoir characterization. In *SEG Annual Technical Conference*, New Orleans, September 1998.

[13] A. S. Hatloy. Numerical facies modeling combining deterministic and stochastic methods. In *Stochastic Modeling and Geostatistics: Principles, Methods, and Case Studies*, J.M. Yarus and R.L. Chambers, editors, pages 109–120. AAPG Computer Applications in Geology, No. 3, 1995.

[14] N. He, A. C. Reynolds, and D. S. Oliver. Three-dimensional reservoir description from multiwell pressure data and prior information. In *1996 SPE Annual Technical Conference and Exhibition Formation Evaluation and Reservoir Geology*, pages 151–166, Denver, CO, October 1996. Society of Petroleum Engineers. SPE Paper Number 36509.

[15] P. Jacquard and C. Jain. Permeability distribution from field pressure data. *SPE Journal*, 5(5):281–294, 1965.

[16] J. L. Landa, M. M. Kamal, C. D. Jenkins, and R. N. Horne. Reservoir characterization constrained to well test data: A field example. In *1996 SPE Annual Technical Conference and Exhibition Formation Evaluation and Reservoir Geology*, pages 177–192, Denver, CO, October 1996. Society of Petroleum Engineers. SPE Paper Number 36511.

[17] D. S. Oliver. Estimation of radial permeability distribution from well test pressure data. *SPE Formation Evaluation*, 7(5):290–296, 1992.

[18] D. S. Oliver. Incorporation of transient pressure data into reservoir characterization. *In Situ*, 18(3):243–275, 1994.

[19] B. S. RamaRao, A. M. LaVenue, G. de Marsily, and M. G. Marietta. Pilot point methodology for automated calibration of an ensemble of conditionally simulated transmissivity fields, 1. Theory and computational experiments. *Water Resources Research*, 31(3):475–493, 1995.

[20] A. C. Reynolds, L. Chu, and D. S. Oliver. Reparamerterization techniques for generating reservoir descriptions conditioned to variograms and well-test pressure. In *1995 SPE Annual Technical Conference and Exhibition Formation Evaluation and Reservoir Geology*, pages 609–624, Dallas, TX, October 1995. Society of Petroleum Engineers. SPE Paper Number 30588.

[21] D. W. Vasco, S. Yoon, and A. Datta-Gupta. Integrating dynamic data into high resolution reservoir models using streamline-based analytic sensitivity coefficients. In *1998 SPE Annual Technical Conference and Exhibition Formation Evaluation and Reservoir Geology*, pages 189–203, New Orleans, LA, September 1998. Society of Petroleum Engineers. SPE Paper Number 49002.

[22] X. H. Wen. *Stochastic Simulation of Groundwater Flow and Mass Transport in Heterogeneous Aquifers: Conditioning and Problem of Scales*. PhD thesis, Polytechnic University of Valencia, Valencia, Spain, 1996.

[23] X. H. Wen, A. S. Cullick, and C. V. Deutsch. Constraints on the spatial distribution of permeability due to a single well pressure transient test. In *Report 10, Stanford Center for Reservoir Forecasting*, Stanford, CA, May 1997.

[24] X. H. Wen, C. V. Deutsch, and A. S. Cullick. High resolution reservoir models integrating multiple-well production data. In *1997 SPE Annual Technical Conference and Exhibition Formation Evaluation and Reservoir Geology*, pages 115–129, San Antonio, TX, October 1997. Society of Petroleum Engineers. SPE Paper Number 38728.

[25] X. H. Wen, C. V. Deutsch, and A. S. Cullick. High resolution reservoir models integrating multiple-well production data. *SPEJ*, 3(4):344–355, 1998.

[26] X. H. Wen and J. J. Gómez-Hernández. Upscaling of hydraulic conductivity in heterogeneous media: An overview. *Journal of Hydrology*, 183(1-2):ix–xxxii, 1996.

[27] X. H. Wen, J. J. Gómez-Hernández, J. E. Capilla, and A. Sahuquillo. The significance of conditioning on piezometric head data for predictions of mass transport in groundwater modeling. *Math. Geology*, 28(7):961–968, October 1996.

[28] W. Xu and A. G. Journel. GTSIM: Gaussian truncated simulations of reservoir units in a West Texas carbonate field. SPE Paper Number 27412, 1993.